Ocean Sci., 12, 1033–1048, 2016
www.ocean-sci.net/12/1033/2016/
doi:10.5194/os-12-1033-2016

Ocean Science Open Access EGU

Assessing the potential for dimethylsulfide enrichment at the sea surface and its influence on air–sea flux

Carolyn F. Walker[1], Mike J. Harvey[1], Murray J. Smith[1], Thomas G. Bell[2,3], Eric S. Saltzman[3], Andrew S. Marriner[1], John A. McGregor[1], and Cliff S. Law[1,4]

[1]National Institute of Water and Atmospheric Research, Wellington, New Zealand
[2]Plymouth Marine Laboratory, Plymouth, UK
[3]University of California Irvine, Irvine, USA
[4]Department of Chemistry, University of Otago, Dunedin, New Zealand

Correspondence to: Carolyn F. Walker (carolyn.walker@royalsociety.org.nz) and Cliff S. Law (cliff.law@niwa.co.nz)

Received: 6 May 2016 – Published in Ocean Sci. Discuss.: 19 May 2016
Revised: 18 July 2016 – Accepted: 4 August 2016 – Published: 5 September 2016

Abstract. The flux of dimethylsulfide (DMS) to the atmosphere is generally inferred using water sampled at or below 2 m depth, thereby excluding any concentration anomalies at the air–sea interface. Two independent techniques were used to assess the potential for near-surface DMS enrichment to influence DMS emissions and also identify the factors influencing enrichment. DMS measurements in productive frontal waters over the Chatham Rise, east of New Zealand, did not identify any significant gradients between 0.01 and 6 m in sub-surface seawater, whereas DMS enrichment in the sea-surface microlayer was variable, with a mean enrichment factor (EF; the concentration ratio between DMS in the sea-surface microlayer and in sub-surface water) of 1.7. Physical and biological factors influenced sea-surface microlayer DMS concentration, with high enrichment (EF > 1.3) only recorded in a dinoflagellate-dominated bloom, and associated with low to medium wind speeds and near-surface temperature gradients. On occasion, high DMS enrichment preceded periods when the air–sea DMS flux, measured by eddy covariance, exceeded the flux calculated using National Oceanic and Atmospheric Administration (NOAA) Coupled-Ocean Atmospheric Response Experiment (COARE) parameterized gas transfer velocities and measured sub-surface seawater DMS concentrations. The results of these two independent approaches suggest that air–sea emissions may be influenced by near-surface DMS production under certain conditions, and highlight the need for further study to constrain the magnitude and mechanisms of DMS production in the sea-surface microlayer.

1 Introduction

In remote, relatively pristine marine environments such as the Southern Ocean, the production of aerosols and clouds is predominantly governed by natural sources (McCoy et al., 2015). In order to represent these sources in Earth system models and project their response to climate change, the exchange of volatiles between the atmosphere and ocean requires rigorous constraint.

Dimethylsulfide (DMS) is derived from phytoplankton, and constitutes the largest natural source of non-sea-salt sulfate aerosol to the global troposphere of 10–20 nmol L^{-1} h^{-1} (Simó, 2001; Andreae and Crutzen, 1997), with an estimated annual input of 28.1 Tg *S* (Lana et al., 2011). Once in the atmosphere, DMS reacts to form sulfate aerosol, which acts as a source of cloud condensation nuclei (CCN). It has been hypothesized that DMS-derived aerosols may thus have a significant impact on the radiation budget (Charlson et al., 1987; Andreae and Crutzen, 1997; Ayers and Gillett, 2000), via direct scattering of sunlight and changes to cloud properties. However, more recent experiments highlight additional biogenic sources and pathways for the production of CCN, even in the absence of sulfate aerosol (Quinn and Bates, 2011; Bianchi et al., 2016; Kirkby et al., 2016). Current global flux estimates of DMS are poorly constrained, with estimates varying by as much as a factor of 2 (Lana et al., 2011).

Direct measurements of the air–sea exchange or flux (F) of a gas are challenging, and so F is often computed using an empirically determined gas transfer coefficient (k) and the air–sea concentration disequilibria (ΔC), according to

the equation $F = k\Delta C$ (Liss, 1983). The variability in flux estimates is widely considered to be driven by uncertainties in k (Zemmelink et al., 2004), which have been determined by a variety of methods including field observations using deliberately released tracers (Nightingale et al., 2000; Wanninkhof et al., 2004; Ho et al., 2011), wind and wave tank experiments (McGillis et al., 2000), global oceanic ^{14}C uptake (Sweeney et al., 2007), and simultaneous measurements of waterside gas concentrations and air–sea flux (Huebert et al., 2004; Marandino et al., 2009; Bell et al., 2013). As gas exchange is primarily driven by shear-generated turbulence, k is often parameterized as a function of wind speed (Liss and Merlivat, 1986; Wanninkhof, 1992; Ho et al., 2006). However, gas fluxes are inadequately modelled by wind speed alone (Blomquist et al., 2006; Zemmelink et al., 2004), as other factors such as wave-breaking, sea state (e.g. Woolf, 2005; Asher et al., 1996), rain (e.g. Ho et al., 2000), and surface films (e.g. Schmidt and Schneider, 2011) also influence gas exchange at the sea surface. To enable prediction of gas fluxes for a range of compounds including DMS, the National Oceanographic and Atmospheric Administration (NOAA) Coupled-Ocean Atmospheric Response Experiment (COARE) model has been developed to incorporate many of the above factors. The model has been tuned to (Fairall et al., 2011) and validated against DMS eddy covariance field data (Blomquist et al., 2006; Yang et al., 2011).

The air–sea concentration disequilibria of DMS, and consequently air–sea exchange, are essentially controlled by the concentration in seawater ([DMS]) as atmospheric concentrations are typically at least 2 orders of magnitude lower. However, [DMS] is invariably measured at or below 2 m depth in both discrete and underway modes, and not at the sea-surface microlayer (SSM), the interface where gas exchange occurs. This assumes that there are no significant sources or sinks of DMS between the sample depth and the sea surface.

Dimethylsulfide concentration in the surface mixed layer is generally determined by the biomass, activity, and species composition of phytoplankton that produce dimethylsulfoniopropionate (DMSP), the precursor to DMS (Turner et al., 1988). Intracellular DMSP is regulated by factors such as nutrient availability and ultraviolet radiation dose (Archer et al., 2010; Toole and Siegel, 2004), whereas extracellular DMSP is influenced by grazing and bacterial processing (Yoch, 2002). To date, studies characterizing near-surface [DMS] have shown a decreasing gradient towards the interface, indicative of degassing to the atmosphere (Zemmelink et al., 2005). However, direct measurements of the air–sea flux of DMS by eddy covariance (EC) over coccolithophore-rich North Atlantic waters significantly exceeded those calculated from bulk seawater concentrations (Marandino et al., 2008). This discrepancy between predicted and observed fluxes was attributed to near-surface [DMS] gradients (above latitudes of 55° N; Marandino et al., 2008).

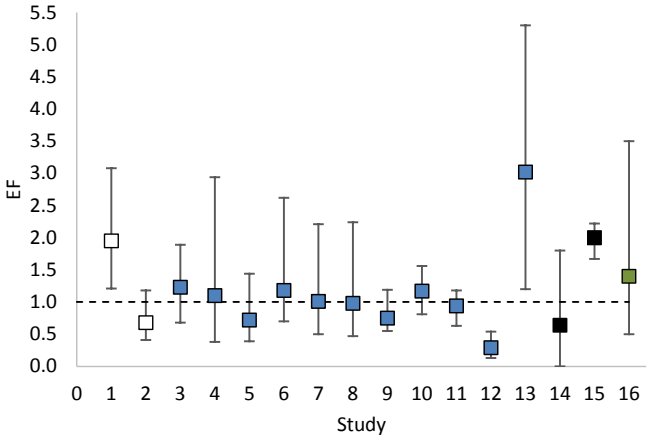

Figure 1. Mean enrichment factors (EFs) for DMS in the SSM reported in previous studies. The upper and lower bars indicate the highest and lowest values reported in each study. An EF of 1.0, shown by the horizontal dashed line, indicates no difference between [DMS_{SSM}] and [DMS_{SSSW}], with EF > 1 denoting enrichment in the SSM relative to SSSW, and values < 1 a deficit relative to SSSW. The sampling method is indicated by the symbol colour: plate (white), mesh (blue), drum (black), and cryogenic (green). References: 1 (Yang, 1999); 2 and 3 (Yang et al., 2001); 4 (Yang and Tsunogai, 2005); 5 (Yang et al., 2005a); 6 (Yang et al., 2005b); 7 (Yang et al., 2006); 8 (Zhang et al., 2008); 9 (Yang et al., 2008); 10 and 11 (Zhang et al., 2009); 12 (Yang et al., 2009); 13 (Matrai et al., 2008); 14 (Zemmelink et al., 2006); 15 (Turner and Liss, 1985); and 16 (Nguyen et al., 1978).

Despite the challenge of maintaining a DMS source in a relatively thin (10–100 µm) layer at the air–water interface that is often subject to extreme physicochemical conditions (Zuev et al., 2001), a number of studies have examined and identified enrichment of DMS in the SSM, as summarized in Fig. 1 and references therein. Sea-surface microlayer thickness, as defined by near-surface biogeochemical gradients, is of the order of 100 µm (Zhang et al., 2003). Given the challenges of sampling this thin surface layer, the thickness has been operationally defined as 1 mm by Liss and Duce (1997). In the current paper we evaluate properties for both 100 µm and 1 mm SSM thicknesses. The physicochemical and biological properties of the SSM are often distinct from underlying waters, and may support enhanced biogeochemical activity (Liss and Duce, 1997). For example, the SSM is often enriched with surface-active organic material and bacteria, and is subject to elevated ultraviolet radiation and temperature (Cunliffe et al., 2013). DMS measurements in the SSM have identified both enrichment and depletion relative to subsurface seawater (SSSW) concentrations; however, enrichment has tended to dominate (Fig. 1). The source and controls of this excess DMS have not been identified, and the assumption that the SSM may influence DMS emissions into the atmosphere remains untested.

A variety of devices have been successfully deployed for sampling biological assemblages and dissolved compounds in the SSM (Cunliffe and Wurl, 2014). Trace gas SSM analyses are more challenging given the difficulties of sampling a volatile gas in a thin film that is subject to airside and waterside turbulence. Indeed, laboratory experiments have shown that a proportion of DMS is inevitably lost during SSM sampling, regardless of the device used (Yang et al., 2001). The aim of the current work was to test the potential for near-surface processes to influence air–sea DMS exchange using a novel combination of direct sampling of the SSM and SSSW, and EC measurement of air–sea DMS flux. Measurements were made during the Surface Ocean Aerosol Production (SOAP) voyage (Bell et al., 2015; Law et al., 2016). The influence of biogeochemical variability on spatial and temporal variation in near-surface DMS enrichment and flux was assessed by measurements in three phytoplankton blooms of differing community composition in productive frontal waters east of New Zealand. This location is currently under-represented in the global DMS database and climatology (Kettle and Andreae, 2000; Lana et al., 2011). In addition, the meteorological and physical factors influencing near-surface [DMS] were also examined in this assessment of DMS enrichment in the SSM, and its potential contribution to air–sea flux.

2 Methodology

2.1 Study location

Sampling was conducted aboard the R/V *Tangaroa* between February and March 2012 along the Chatham Rise, an underwater plateau separating subantarctic and subtropical waters in the south-western Pacific, east of New Zealand. This is a region of high productivity in which frontal activity enhances mixing in the water column, fostering large phytoplankton blooms in the spring and summer seasons (Murphy et al., 2001). Satellite imagery in combination with continuous measurement of surface (6 m depth) chlorophyll *a* fluorescence and seawater [DMS], measured by atmospheric pressure chemical ionization mass spectrometry (API-CIMS; Bell et al., 2015), was used to locate phytoplankton blooms for focussed studies on a range of air–sea parameters during the SOAP voyage (Law et al., 2016). SSM and SSSW sampling was undertaken in three distinct blooms: B1 (DOY 45.8 to 48.8), B2 (DOY 52.8 to 55.0), and B3 (DOY 58.1 to 65.1), located as shown in Fig. 2. Day of year (DOY) is defined as 1 on 1 January 00:00:00 (hh:mm:ss).

2.2 Seawater collection

Near-surface seawater samples were collected from a rigid-hulled inflatable boat (RHIB) during periods of low swell and wind speeds $< 10\,\mathrm{m\,s^{-1}}$. The light wind conditions reduced both DMS loss during collection (Zemmelink et al., 2005) and physical disruption of the in situ SSM (Carlson, 1983). The RHIB was positioned at least 500 m upwind of the R/V *Tangaroa* to avoid ship-borne contamination and artefacts associated with downstream turbulence. A total of 11 SSM stations were sampled, with station coordinates and sampling dates and times shown in Table 1.

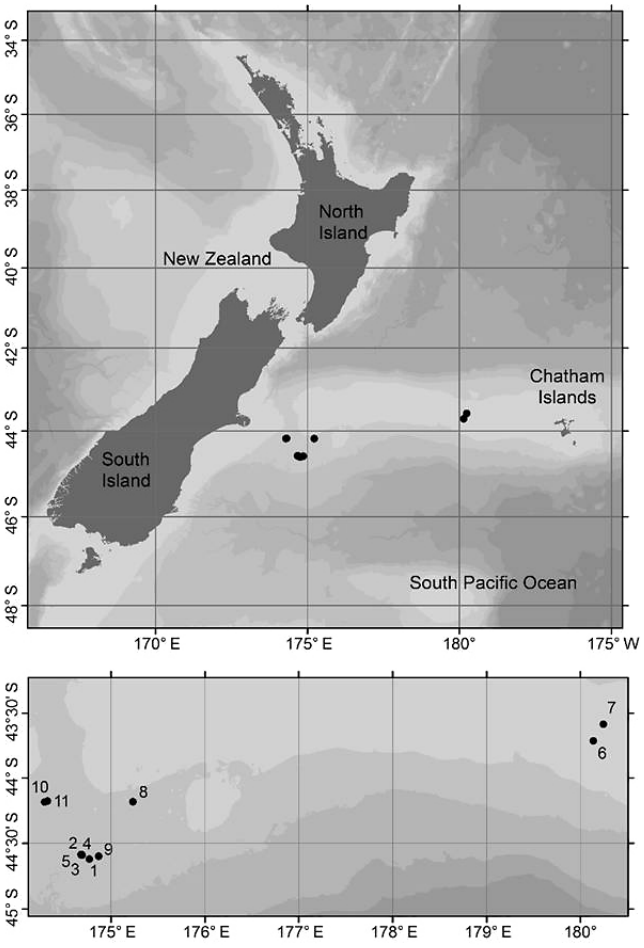

Figure 2. A map of New Zealand waters showing the locations of the 11 SSM sampling stations (solid dots). Station numbers are shown in the expanded Chatham Rise region in the lower panel. Blooms B1, B2, and B3 encompass stations 1–5, 6–7, and 8–11, respectively.

2.2.1 Sea-surface microlayer

A number of devices have been used to sample the SSM, but there have been few comparisons of techniques (Cunliffe and Wurl, 2014, and references therein). In this study the Harvey glass plate (Harvey, 1966; Harvey and Burzell, 1972) and Garrett metal screen (Garrett, 1965) were deployed as these are two of the most frequently used techniques (see Fig. 1). The glass plate works on the principle that the SSM adheres to its surface as it is withdrawn, while the screen relies on surface tension to trap SSM water and matter in the interstitial

Table 1. Sea-surface microlayer station variables: DMS concentrations in the SSM ([DMS_{SSM}]), collected using the plate method, and in seawater at 1.6 m depth ([$DMS_{1.6\,m}$]); DMS enrichment factor (EF); and DMS production rate (PR_{SSM}) for a 100 and 1000 µm thick SSM. EF is the ratio of [DMS_{SSM}] and [$DMS_{1.6\,m}$], with an EF > 1 indicating enrichment and < 1 depletion. Production rates are averages for the period 3 h before and 5 h after SSM sampling. Day of year (DOY) 1 is 1 January 00:00:00. [DMS] errors are 1 SD from the mean of duplicate samples.

DOY UTC	NZDT dd/mm/yy hh:mm	Lat	Long	$[DMS_{1.6\,m}]$ (nM)	$[DMS_{SSM}]$ (nM)	EF	$PR_{SSM\_100\,\mu m}$ ($nmol\,L^{-1}\,h^{-1}$)	$PR_{SSM\_1000\,\mu m}$ ($nmol\,L^{-1}\,h^{-1}$)
B1								
45.8	15/02/12 08:05	44.62° S	174.77° E	4.9 ± 0.8	26.1 ± 0.0	5.3	1153 ± 522	115 ± 52
46.8	16/02/12 08:06	44.59° S	174.68° E	13.6 ± 0.6	25.9 ± 8.2	1.9	−486 ± 270	−49 ± 27
47.1	16/02/12 15:51	44.59° S	174.69° E	13.8 ± n/a	19.9 ± n/a	1.4	n/a	n/a
47.8	17/02/12 08:02	44.59° S	174.69° E	9.2 ± 2.0	41.5 ± 9.7	4.5	5529 ± 655	553 ± 66
48.8	18/02/12 08:04	44.59° S	174.69° E	5.9 ± 0.4	4.1 ± 0.2	0.7	2468 ± 454	247 ± 45
Mean				9.5 ± 4.2	23.5 ± 13.5	2.8	2166 ± 2546	217 ± 255
B2								
52.8	22/02/12 08:27	43.72° S	179.86° W	6.9 ± 0.2	8.7 ± 1.1	1.3	−1445 ± 348	−145 ± 35
55.0	23/02/12 13:03	43.59° S	179.75° W	7.1 ± 1.8	7.0 ± 0.0	1.0	−153 ± 52	−15.3 ± 5
Mean				7.0 ± 0.1	7.9 ± 1.2	1.2	−799 ± 914	−80 ± 91
B3								
58.1	27/02/12 14:39	44.11° S	175.14° E	8.7 ± 0.0	5.0 ± 0.2	0.6	614 ± 162	61 ± 16
59.8	29/02/12 08:03	44.60° S	174.87° E	6.6 ± 0.9	3.8 ± 0.4	0.6	867 ± 129	87 ± 13
64.8	05/03/12 09:04	44.18° S	174.33° E	10.5 ± 0.1	10.2 ± 1.1	1.0	n/a	n/a
65.1	05/03/12 14:12	44.18° S	174.33° E	6.3 ± 0.0	7.1 ± 0.8	1.1	n/a	n/a
Mean				8.0 ± 2.0	6.5 ± 2.8	0.8	740 ± 179	74 ± 18

n/a = data that is not available.

spaces within a wire grid. The surface areas of the rectangular plate and round screen (with 0.6 mm wires) were 600 and 804 cm^2, respectively. The glass plate was silanized to avoid DMS loss through surface adsorption. Samplers were inserted vertically into the sea surface on the downwind side of the boat where the SSM was less disturbed. The plate was slowly removed in the vertical position, whereas the screen was rotated 90° while submerged and then removed at a near-horizontal angle. Seawater adhering to the collection device was immediately drained through a funnel into prewashed 30 ml glass serum bottles for 30 s. Although a wiper is often used with the plate for sampling particulates and surfactants (Cunliffe and Wurl, 2014), this was not used in the current study to avoid DMS loss and potential disruption of algal cells. DMS concentrations in the SSM are referred to herein as [DMS_{SSM}].

2.2.2 Sub-surface water

In addition to the SSM, seawater for the determination of [DMS] was collected in duplicate from four sub-surface depths (< 1, 7, 30, and 162 cm) in 150 mL crimp-top glass bottles that were pre-washed in a solution of phosphate-free detergent and rinsed with ultrapure water. Seawater from just below the SSM was collected using a "sipper", with seawater pumped from a network of floating silicone tubes (each ∼ 300 mm long and with a 3.2 mm outer diameter) using a peristaltic pump into a collection bottle. The tube intake ends were slightly weighted, to minimize disturbance of the SSM and air bubble introduction, for sampling at a depth of 1–2 cm that precluded the SSM. Seawater from depths of 7, 30, and 162 cm was collected using three fixed-depth stainless steel tubes attached to a floating buoy and connected to a peristaltic pump. Samples from 162 cm (referred to herein as [$DMS_{1.6\,m}$]) were assessed for pump-associated artefacts by comparison with samples collected at 2 m depth using standard Niskin bottles on a CTD rosette. The latter was collected within 1 h of the RHIB sampling. A Wilcoxon signed-ranks test for paired samples with non-parametric distributions indicated no significant ($p = 1, \alpha = 0.5$) difference between the two approaches.

Phytoplankton identification, biomass, and abundance data were obtained by optical microscopy of Lugol's preserved samples.

2.3 Analytical methods

2.3.1 Seawater DMS (continuous)

Dimethylsulfide concentration was continuously measured in the ships' seawater intake (at 6.0 m depth; [$DMS_{6.0\,m}$]) using an atmospheric pressure chemical ionization mass spectrometer equipped with a porous membrane equilibrator, UCI miniCIMS (Bell et al., 2013). The miniCIMS data were averaged over 5 min and have a mean relative standard error of ±5 %. A 1 h moving average algorithm was used to further smooth [$DMS_{6.0\,m}$].

2.3.2 Seawater DMS (discrete)

Discrete seawater samples were analysed for DMS while at sea using a semi-automated purge and trap system with a HP 6850 gas chromatograph interfaced with an Agilent flame photometric detector (Walker et al., 2000) up until DOY 47.0. An Agilent (Sievers) 355 sulfur chemiluminescent detector (SCD) was used after DOY 47.0. Seawater samples were gently filtered through an inline 25 mm GF/F filter to remove particulates, and a calibrated volume (5 mL) of the filtrate transferred to a 10 mL silanized glass chamber fitted with a quartz frit and purged with zero-grade nitrogen (99.9 % pure). The chamber and frit were cleaned daily with 5 % HCl and ultrapure water to prevent organic matter build-up. The GF/F filter was changed between each sample and the filter holder rinsed with ultrapure water. Gas-phase DMS was cryogenically concentrated on 60/80 Tenax® TA in a 1/8″ Restek Sulfinert®-treated stainless steel trap at −20 °C and thermally desorbed at 100 °C for GC analysis.

Calibration was carried out using two temperature-controlled VICI® Metronics wafer permeation tubes, one filled with methylethylsulfide (MES) and the other with DMS. MES was used as an internal standard, with samples doped during analysis to allow for correction of short-term changes in detector sensitivity. The DMS permeation tube, housed in a Dynacalibrator®, provided the external standard. A five-point calibration was performed twice per day, and a running standard every 12 samples. A subsequent international intercalibration (Swan et al., 2014) indicated that the analytical method was 93.5 ± 3.8 % accurate with 2.6 % variation. Blank samples were tested regularly, using both ultrapure water and DMS-free seawater from a depth of 500 m, with a mean blank of < 0.1 nmol L^{-1} DMS.

Water samples were analysed within 5 h of collection. Throughout the voyage, the SCD and miniCIMS techniques were compared using seawater from the ship's intake system. The SCD technique gave slightly higher concentrations, with the mean of the residuals indicating an average difference of 1.2 nmol L^{-1} DMS (Fig. 3). This difference is possibly attributable to DMS production during sample storage prior to SCD analysis, as deck incubation of SSSW and SSM water from B2 and B3 indicated mean in-bottle production rates

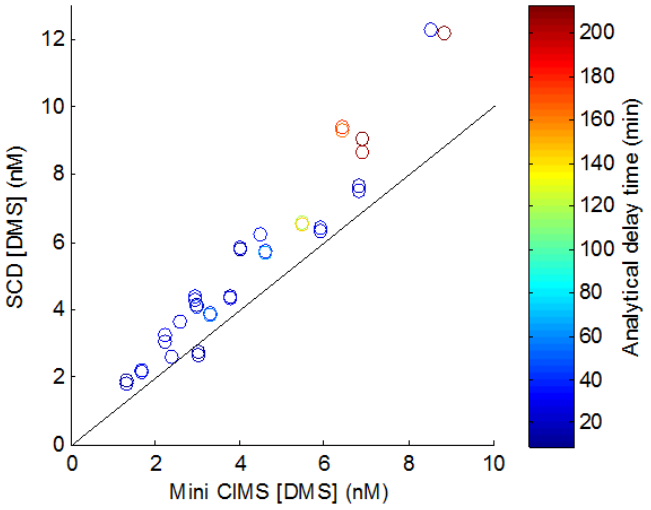

Figure 3. Comparison between [DMS] measured using the miniCIMS and SCD methods. The colour bar indicates the time elapsed between sample collection and analysis on the SCD. MiniCIMS analysis was near real time, so data are averaged over a 1 h period surrounding the SCD sample collection time. The black solid line is 1 : 1.

in the dark of 0.23 nmol L^{-1} h^{-1} (Cliff Law, personal communication, 2016): a total production of 1.2 nmol L^{-1} over 5 h. In addition, the pattern of deviation from the 1 : 1 line of [DMS] in samples with both low and high storage times suggests storage time is not a significant driver of the difference between the two analytical techniques (Fig. 3). Further investigation also showed a lack of relationship between analysis time and EF, particularly for B1 samples ($r^2 = 0.002$), suggesting that there was no significant DMS production between collection and analysis.

2.3.3 SSM enrichment factors

The anomaly between the SSM and underlying SSSW is indicated by the enrichment factor (EF), the concentration ratio between DMS in the SSM and at 1.6 m depth:

$$\mathrm{EF} = \frac{[\mathrm{DMS_{SSM}}]}{[\mathrm{DMS_{1.6m}}]}, \quad (1)$$

EFs were calculated using [$DMS_{1.6\,m}$] from the RHIB rather than [$DMS_{6.0\,m}$] from the ship's seawater intake, to minimize error arising from spatio-temporal variability. An EF > 1 indicates DMS enrichment and < 1 indicates DMS depletion, in the SSM.

2.3.4 Eddy-covariance-derived DMS air–sea flux

Although the basic principles of turbulent flux exchange are well established (Swinbank, 1951), refinements have been made to adapt the micrometeorological technique of EC for use on a moving platform (e.g. Edson et al., 1998). In addi-

tion, the development of atmospheric pressure chemical ionization mass spectrometry (API-CIMS) for high-frequency DMS measurement (Bandy et al., 2002; Huebert et al., 2004; Marandino et al., 2007) has enabled direct measurements of air–sea DMS flux on timescales of the order of tens of minutes. By combining airside and waterside gas concentrations, these high-resolution measurements allow the response of k in relation to spatial variation in biological and environmental conditions to be determined. In the current study, continuous measurement of air–sea DMS flux at 10 min intervals on the ship's bow was achieved using EC and API-CIMS, as described in Bell et al. (2013). EC flux data (F_{EC}) were smoothed using a moving average algorithm with a span of 1 h and used to calculate the inferred DMS concentration in surface waters (see Sect. 2.4.2).

2.3.5 Near-surface temperature gradients

A spar buoy was deployed in each bloom for autonomous sampling of near-surface temperature gradients. Temperature loggers (RBR TR-1060) recorded temperature at 0.5 m intervals between 0.25 and 4.25 m depth, with deployments typically lasting 4 days.

2.4 Computations

2.4.1 Air–sea DMS fluxes

DMS flux (F_{DMS}) was calculated using the gas transfer coefficient k and the concentration difference at the air–sea interface according to

$$F_{DMS} = k(C_w - \frac{C_a}{H}), \quad (2)$$

where H is the dimensionless Henry's law solubility coefficient for DMS (Dacey et al., 1984), C_w is [$DMS_{6.0\,m}$], and C_a is the DMS concentration measured in air. Most conceptual models assume that k is dependent on molecular diffusion across the surface layer, the thickness of which is modulated by near-surface turbulent processes (Liss and Slater, 1974). For DMS in temperate waters, the waterside diffusive layer provides the dominant control on air–sea flux. This assumes there is no significant internal loss or production in the thin diffusive layer at the surface (Nightingale, 2013), and also that there is more rapid mixing below. The transfer velocity k was calculated using the NOAA COARE model (version 3.1g; Fairall et al., 2011) and parameterized in terms of local wind speed scaled to 10 m height, as in Bell et al. (2015). k was then adapted for DMS using the Schmidt number for local seawater temperature and salinity at 6.0 m depth (Saltzman et al., 1993).

2.4.2 Flux-inferred seawater [DMS]

The inferred DMS concentration in surface waters required to support the observed air–sea flux ([DMS_{inf}]) was derived from Eq. (2) using the measured EC flux, F_{EC}, and a k predicted by the NOAA COARE model, which incorporates bulk meteorological variables including wind speed, temperature, and stability (Bell et al., 2015). To generate [DMS_{inf}] at the same sampling frequency as the smoothed [$DMS_{6.0\,m}$], k was calculated at 10 min intervals and smoothed using a moving average algorithm with a span of 1 h. To facilitate comparison with [DMS_{SSM}], a mean [DMS_{inf}] was generated for each RHIB station for the period 3 h before SSM sampling until 5 h afterwards.

2.4.3 DMS production in the SSM

The excess or residual [DMS] in the SSM, relative to underlying waters, was calculated using two independent approaches. Subtracting [$DMS_{1.6\,m}$] from [DMS_{SSM}] provided an estimate of SSM-derived residual [DMS], the excess [DMS] in the SSM determined by direct measurement. A second approach was to subtract the observed [$DMS_{6.0\,m}$] from the estimated [DMS_{inf}] to derive an estimate of EC-derived residual [DMS], the excess [DMS] in the SSM calculated indirectly from flux measurements. The latter was used to estimate the net DMS production rate in the SSM (PR_{SSM}) required to support the observed air–sea flux:

$$PR_{SSM} = \frac{F_{EC} - F_{6.0\,m}}{z}, \quad (3)$$

where F_{EC} is the flux measured by EC, $F_{6.0\,m}$ is the flux estimated using [$DMS_{6.0\,m}$] and Eq. (2), and z is the SSM thickness (10 µm and 1 mm). As PR_{SSM} was calculated using the measured and expected DMS flux, it is independent of the measured [DMS_{SSM}].

3 Results

3.1 Comparison of SSM sampling techniques

Comparison of [DMS_{SSM}] measured by the Garret metal screen and Harvey glass plate, using a Wilcoxon signed-ranks test for paired samples, indicated a significant difference in results ($p = 0.0078$, $\alpha = 0.05$), with mean [DMS_{SSM}] from plate sampling 42 % lower than that from the Garret screen. This difference was substantially greater than the sampling blanks, which were determined using both ultrapure water and seawater from 500 m depth (consistently < 0.3 nmol L^{-1} DMS for both devices; 1.6 % of the average sample concentration). One potential factor is that the Garret screen collects thicker SSM samples than the plate (Cunliffe and Wurl, 2014); however, there are also other differences in collection efficiency between the two methods. The screen is considered to recover more of the phytoplankton assemblage than the plate (Momzikoff et al., 2004; Agogué et al., 2004). In the current study, the screen appeared to trap aggregates, particularly in B1, and this may have led to overestimates of [DMS_{SSM}]. Consequently, we will only discuss SSM data

collected using the plate method, as these provide more conservative estimates of DMS enrichment in the SSM.

3.2 Direct measurements of [DMS] in the SSM and SSSW

Dimethylsulfide concentrations in the SSM and [$DMS_{1.6\,m}$] ranged from 3.8 to 41.5, and 4.9 to 13.8 nmol L^{-1}, respectively (Table 1, Fig. 4), and showed similar spatial variability to [$DMS_{6.0\,m}$] (Fig. 5b, Bell et al., 2015). Maximum concentrations were observed in B1 (DOY 45.8 to DOY 48.8), with mean [DMS_{SSM}] and [$DMS_{1.6\,m}$] of 23.5 ± 13.5 and 9.5 ± 4.2 nmol L^{-1}, respectively, coincident with a mean [$DMS_{6.0\,m}$] of 10.6 ± 5.2 nmol L^{-1} (range 2.9–24.7 nmol L^{-1}). B1 was dominated by dinoflagellates (Law et al., 2016), with a mean chlorophyll *a* of 1.6 mg m^{-3} at 1–2 cm depth. A striking feature of B1 was the high [DMS_{SSM}], which exceeded [$DMS_{6.0\,m}$] (Fig. 5b), resulting in high average EFs (2.8 ± 2.0, Table 1). Furthermore, two B1 stations exhibited EFs >4.0, which exceed the majority of [DMS_{SSM}] maxima reported in the literature (Fig. 1). Conversely, B2 and B3 were characterized by lower [DMS_{SSM}], which was typically indistinct from [$DMS_{6.0\,m}$] (see Fig. 5b). The mean [DMS_{SSM}] and [$DMS_{1.6\,m}$] in B2 were 7.9 ± 1.2 and 7.0 ± 0.1 nmol L^{-1}, respectively, with near-surface seawater at 1–2 cm depth of 1.0 mg m^{-3} chlorophyll *a*, ∼ 40 % lower than B1, and dominated by coccolithophores. Although B3 was in a similar location to B1, it was temporally distinct and with lower phytoplankton biomass (Law et al., 2016). Near-surface seawater was dominated by dinoflagellates and coccolithophores, with mean chlorophyll *a*, [DMS_{SSM}], and [$DMS_{1.6\,m}$], of 0.8 mg m^{-3}, 6.5 ± 2.8, and 8.0 ± 2.0 nmol L^{-1}, respectively, and EFs near or below 1.0. Throughout the study there was no evidence of near-surface [DMS] gradients between 1 cm and 1.6 m depth, including at the B1 stations exhibiting high levels of SSM enrichment (Fig. 4). The absence of near-surface DMS gradients was further confirmed by the agreement between [$DMS_{1.6\,m}$] and [$DMS_{6.0\,m}$] (Fig. 5b).

3.3 Flux-inferred estimates of [DMS]

The air–sea flux of DMS measured by EC, F_{EC}, was elevated during B1, with fluxes up to ∼ 100 µmol m^{-2} d^{-1} (Bell et al., 2015). The highest DMS fluxes were recorded between DOY 48.0 and 50.0 during B1, reflecting the elevated [$DMS_{6.0\,m}$] (Fig. 5b, Bell et al., 2015). The inferred DMS concentration in SSSW required to support the F_{EC}, [DMS_{inf}], was calculated using NOAA COARE gas transfer coefficients and compared to [$DMS_{6.0\,m}$] (Fig. 5b). DMS concentrations measured at 6.0 m depth were used to represent SSSW, since continuous measurement at this depth provided greater temporal resolution (Bell et al., 2015). Overall, comparison of [DMS_{inf}] and [$DMS_{6.0\,m}$] in Fig. 5b shows good agreement. Where [DMS_{inf}] and [$DMS_{6.0\,m}$] agree in magnitude (e.g.

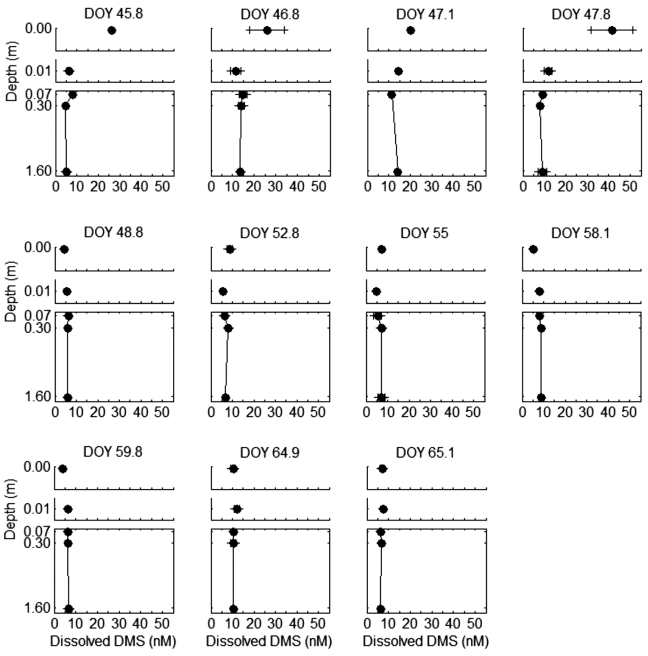

Figure 4. Near-surface gradients of [DMS] in the SSM and in the upper 1.6 m. Measurements presented are the mean replicate samples, and error bars represent 1 standard deviation.

DOY 55.0 to 58.0) the application of [$DMS_{6.0\,m}$] and *k* provides a robust estimate of air–sea DMS flux. However, between DOY 44.8 and 52.0, and to a lesser extent between DOY 58.0 and 61.0, a disparity was apparent with anomalously high [DMS_{inf}] observed that were not reflected in [$DMS_{6.0\,m}$]. During these periods, the use of [$DMS_{6.0\,m}$] with *k* would underestimate the DMS flux. This disparity is evident during B1 in the comparison of EC- and SSM-derived residual [DMS], with the maxima of these independent approaches appearing close to each other (Fig. 5c). EC- and SSM-derived residual [DMS] were significant during B1 occupation, with maximum values of 20 and 33 nmol L^{-1}, respectively, during Station 4 (DOY 47.7 to 48.1), whereas EC- and SSM-derived residual [DMS] were generally not significant in B2 and B3.

These trends are confirmed by comparison of [$DMS_{6.0\,m}$] and [DMS_{inf}] for each bloom period in Fig. 6a–c. B1 shows a positive anomaly in [DMS_{inf}] relative to [$DMS_{6.0\,m}$], particularly at elevated [$DMS_{6.0\,m}$], indicative of an additional source of DMS contributing to the flux. At two of the four stations during B1, the mean [DMS_{inf}] was significantly greater than the mean [$DMS_{6.0\,m}$], with this positive bias in [DMS_{inf}] in B1 generally highest at intermediate wind speeds (Fig. 6a). Conversely, B2 and B3 generally showed good agreement between [DMS_{inf}] and [$DMS_{6.0\,m}$], although there was evidence of a negative anomaly at low to intermediate wind speeds (Fig. 6b–c) and a positive anomaly at high wind speeds in B3 (Fig. 6c). Comparison of the mean

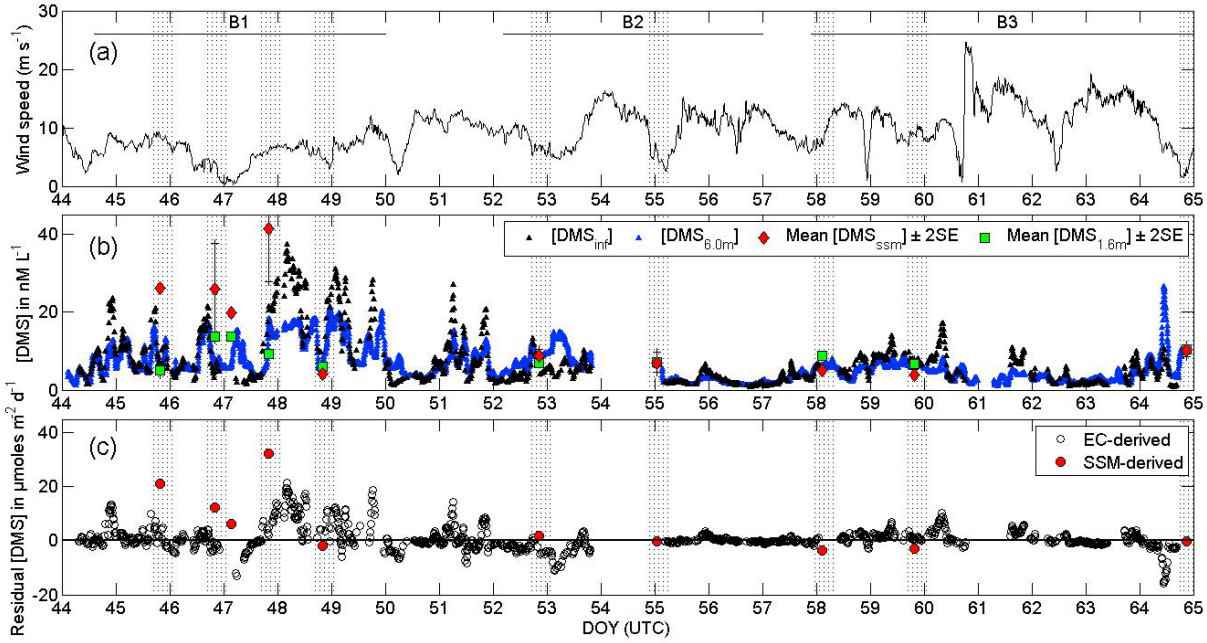

Figure 5. **(a)** Wind speed normalized to 10 m. **(b)** Flux-inferred concentrations of seawater DMS, [DMS_{inf}] (black triangles), overlain with the mean for [DMS_{SSM}] (red diamonds), [$DMS_{1.6\,m}$] (green squares), and [$DMS_{6.0\,m}$] (blue triangles). [DMS_{inf}] was calculated from continuous EC flux measurements and COARE k values based on local conditions. [DMS_{inf}] and [$DMS_{6.0\,m}$] data sets were smoothed using a moving average algorithm with a span of 1 h. Error bars indicate 2× standard error of the mean of replicate samples. Shaded areas indicate the period from 3 h prior to and 5 h after SSM sampling. Periods encompassing intense sampling within algal blooms (B1, B2, and B3) are indicated by the horizontal lines at the top of the graph. Sea-surface microlayer measurements for DOY 47.1 and 64.8 coincide with a gap in EC air–sea flux data. On DOY 48.8, changes in [$DMS_{6.0\,m}$] during station occupation indicate the SSM sample is unlikely to be representative of the SSM for the entire station. **(c)** SSM-derived residual [DMS] (solid red circles) compared with EC-derived residual [DMS] (solid black circles).

EC- and SSM-derived residual [DMS] for each station confirmed that the B2 and B3 stations generally cluster around the zero intercept (Fig. 6d), as expected if near-surface DMS sources were negligible. Conversely, B1 stations exhibited significant deviation from the zero intercept, with two stations characterized by high EC- and SSM-derived residual [DMS] coincident with high EF. At both of these stations the SSM-derived residual [DMS] exceeded the EC-derived residual [DMS], which may reflect the spatial variability of DMS in the SSM, non-representativeness of the single-point SSM measurements, or methodological artefacts.

3.4 Meteorological influences on near-surface structure

Bloom 1 was sampled during a high-pressure system with low wind speeds (mean $6.0 \pm 2.7\,m\,s^{-1}$; Figs. 5a and 7) and calm sea state (waves < 0.2 m), conditions conducive to SSM formation and preservation. A brief atmospheric front traversed the region during B2 with winds reaching $18\,m\,s^{-1}$, and multiple weather fronts occurred during B3 including a period of sustained high wind speeds up to $30\,m\,s^{-1}$ (Fig. 5a). At wind speeds $> 10\,m\,s^{-1}$ the SSM is disrupted, with its constituents dispersed and diluted by sub-surface water (Wurl et al., 2011), and ventilation increases. The influence of physical processes on a potential SSM source of DMS was examined between DOY 45.5 and 49.5 in B1 by comparison of EC- and SSM-derived residual [DMS] with U_{10} (wind speed at a reference height of 10 m above the ocean) and near-surface temperature gradient (Fig. 7). Low wind speeds reduce air–sea exchange and enhance near-surface stratification, providing optimal conditions for maintenance of the SSM and retention of DMS. If this is the case, then the contribution of the SSM to DMS flux would be most significant when the SSM is subsequently ventilated upon an increase in wind speed. This scenario is apparent on DOY 47.0 to 48.0, when a period of low wind speeds ($< 3\,m\,s^{-1}$), significant near-surface temperature gradients ($\sim 1\,°C\,m^{-1}$), and elevated SSM-derived residual [DMS] was followed by a period of higher wind speed (~ 5–$8\,m\,s^{-1}$), during which the EC-derived residual [DMS] increased (Fig. 7). However, the high SSM-derived residual [DMS] was also recorded at wind speeds of 6–9 $m\,s^{-1}$ during DOY 45.8, indicating that DMS enrichment in the SSM may be maintained at moderate wind speeds.

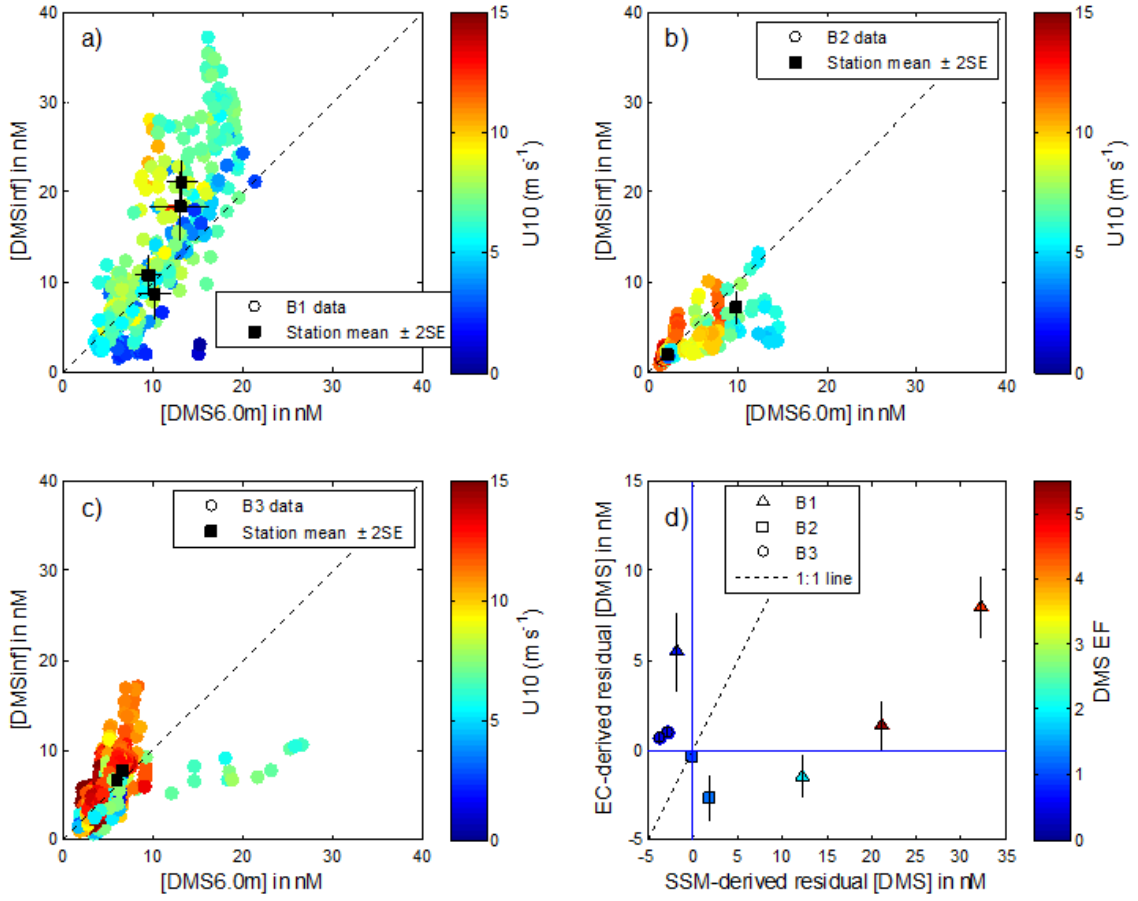

Figure 6. (a–c) Comparison between smoothed [DMS_{inf}] and [$DMS_{6.0\,m}$] (10 min intervals) during each bloom period. The black dashed line indicates the 1 : 1 relationship. The black squares indicate the mean during the period from 3 h prior to 5 h post-sampling the SSM, with error bars indicating 2× the standard error. The symbol colour indicates wind speed (U_{10}), as shown in the colour bar. **(d)** Relationship between SSM-derived residual [DMS] and EC-derived residual [DMS] for each SSM station. Data are not available for stations sampled on DOY 47.1, 64.8, and 65.1. Solid vertical and horizontal lines indicate zero residual [DMS] and the dashed line indicates the 1 : 1 relationship. The symbol colour indicates the enrichment factor (EF). The periods used to calculate station means are denoted by shading in Fig. 5.

3.5 DMS production rates in the SSM

The SSM production rate, PR_{SSM}, was estimated by subtracting the expected flux, calculated using [$DMS_{6.0\,m}$] and the COARE algorithm, from the observed air–sea flux, and dividing by the thickness of the SSM (Eq. 3). This approach assumes that DMS production in the SSM was the source of the "excess" air–sea flux in B1. Other potential DMS loss processes, such as photolysis and bacterial oxidation, may have also been significant DMS sinks (Kieber et al., 1996; Gali et al., 2013); however, as these rates were not quantified they are not considered, and so the estimate of PR_{SSM} may represent an underestimate.

Mean PR_{SSM} was estimated using SSM thicknesses of 100 and 1000 µm. Assuming a thickness of 1000 µm, PR_{SSM} was 217 ± 162, -80 ± -33, and 74 ± 22 for stations B1, B2, and B3, respectively (Table 1). An alternative SSM thickness of 100 µm resulted in PR_{SSM} 1 order of magnitude higher. The large uncertainty for each estimate is partially attributable to variation in the measured F_{EC} and [$DMS_{6.0\,m}$] (see Fig. 5b). This approach of estimating PR_{SSM} from flux measurements has several advantages in that it is independent of the measured [DMS_{SSM}], integrates horizontal variability, eliminates inherent uncertainty in the wind speed–gas transfer relationship, and does not rely on a single-point SSM measurement.

4 Discussion

The results of two independent techniques to assess the potential contribution of the SSM to the air–sea exchange of DMS provide intriguing evidence that this may be significant under certain physical and biological conditions. This study adds to a number of other reports of DMS enrichment in the SSM (Fig. 1), but raises challenging questions regarding the source and maintenance of elevated DMS in the SSM. Consequently it is instructive to consider the validity of these

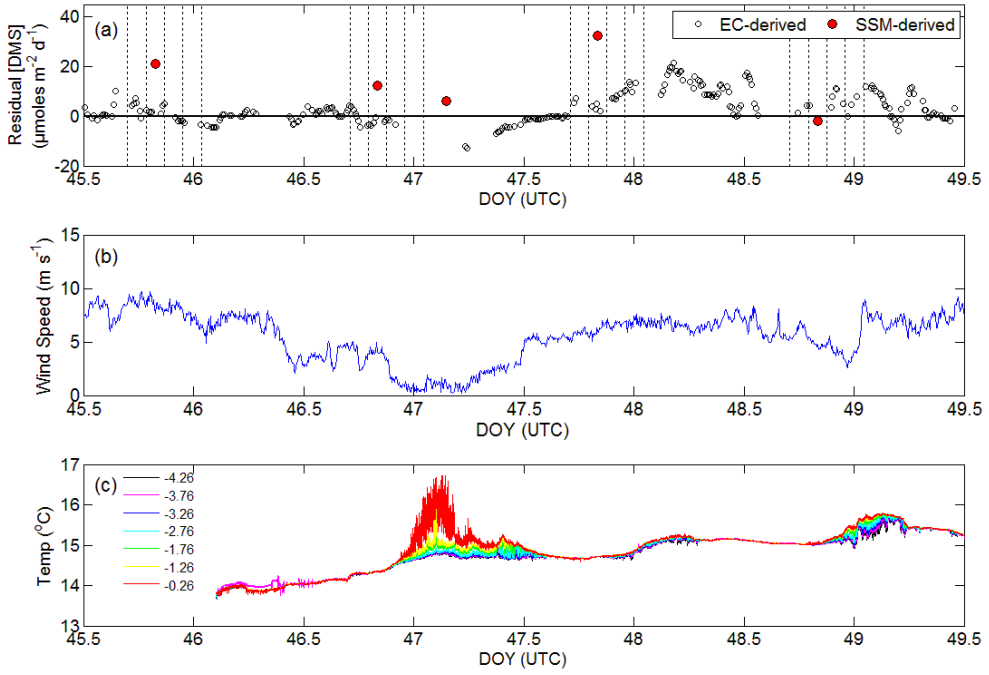

Figure 7. The period between DOY 45.5 and 49.5 in Bloom 1 showing **(a)** SSM-derived residual [DMS] (solid red circles) and EC-derived [DMS] (open black circles). SSM measurements for DOY 47.1 coincided with a gap in EC air–sea flux data. Vertical dashed lines indicate the period from 3 h before to 5 h after sampling (not shown for DOY 47.1). **(b)** Wind speed normalized to 10 m. **(c)** Near-surface temperatures (legend shows depth in metres).

results and the physical and biological factors that may influence DMS in the SSM.

Near-surface gradients in dissolved gases have been reported previously for DMS and carbon dioxide (Zemmelink et al., 2005; Calleja et al., 2005), with potential implications for air–sea flux estimates. The vertical DMS profile in near-surface waters in B2 and B3 was uniform (see Fig. 4), indicating that DMS production and loss terms, such as ventilation, bacterial oxidation, and photolysis, were in balance (Galí et al., 2013). Furthermore, the profiles do not show significant near-surface depletion in [DMS], which has been previously reported and attributed to ventilation and photolysis (Kieber et al., 1996).

The presence of significant DMS enrichment in the SSM at the B1 stations (Table 1) is surprising, as vertical diffusion from the SSM would be expected to elevate [DMS] immediately below the SSM. As elevated [DMS] was not apparent at 1–2 cm (Fig. 4), this suggests that density stratification and/or preferential retention of DMS in the SSM suppressed vertical diffusive losses from the SSM. Elevated [DMS_{SSM}] has been previously reported relative to concentrations at 25 cm depth, associated with near-surface density gradients arising from ice melt in the Weddell Sea (Zemmelink et al., 2005). The near-surface temperature data in the current study indicated episodic formation of a gradient in the upper 4 m at the B1 stations (see Fig. 7) and, assuming this gradient extended to the sea surface, the resulting stratification may have created optimal conditions for SSM enrichment, with concentration and retention of phytoplankton whilst suppressing diffusive loss to sub-surface water. Furthermore, if surfactants were present they may have suppressed ventilation across the air–sea interface (Salter et al., 2011) under these conditions, leading to an accumulation of DMS in the SSM.

The sea-surface microlayer sampling, storage, and analysis may have introduced potential artefacts, particularly for trace gases. The mesh screen sampling produced higher [DMS_{SSM}] than the plate, potentially due to preferential retention of algal and suspended material on the mesh as previously reported (Turner and Liss, 1985). These authors also reported significant DMS enrichment coincident with elevated sub-surface productivity, and partially attributed the enrichment to "stressing of SSM organisms as a result of the sampling procedure". This may have occurred in the current study in B1, as dinoflagellates are sensitive to shear stress (Wolfe et al., 2002), but this was not tested. However, in contrast to other applications (Cunliffe and Wurl, 2014), we avoided scraping the SSM off the glass plate to reduce transfer of particulate material and ventilation of DMS, and this may also have reduced shear stress and exposure time of the phytoplankton. Exposure to air during SSM sampling enhances DMS evasion, with ∼ 50 % loss at zero wind speed (Zemmelink et al., 2005), which suggests that the majority of previous DMS measurements in the SSM (see Fig. 1) are underestimates (Zemmelink et al., 2006).

This raises the question as to how DMS enrichment is maintained in the SSM whilst ventilation is occurring across the air–sea interface. Zemmelink et al. (2006) calculated a DMS residence time in the SSM of the order of 40–60 s, and consequently a very high production rate would be required to maintain enrichment.

To maintain the observed and calculated enrichment in the SSM, DMS production must dominate over loss terms such as photolysis and bacterial oxidation and occur at a significantly greater rate than previously reported for the open ocean. Indeed, the PR_{SSM} estimates in Table 1, which are determined indirectly from F_{EC} and are independent of the SSM concentration measurements, significantly exceed reported DMS production rates for sub-surface waters (Simó, 2004). For example, in a compilation of 65 studies the maximum gross DMS production rates of 10–20 nmol L^{-1} h^{-1} (Simó, 2004) were up to 2 orders of magnitude lower than the calculated PR_{SSM} based upon a 1000 µm SSM thickness.

Microorganisms in the SSM are exposed to extreme physicochemical conditions, including high irradiance (Zuev et al., 2001), whereas the DMS production rate estimates reported in Simó (2004) were from dark incubations that exclude the influence of light on DMS production. The conversion of intracellular DMSP to DMS is considered to be sensitive to both the quantity and spectra of light (Sunda et al., 2002; Archer et al., 2010), and so exposure to high irradiance in the SSM will have a significant influence on DMS production. This is supported by the "DMS summer paradox" where higher DMSP and DMS levels have been observed in shallow mixed layers that are exposed to high light levels (Simó and Pedrós-Alió, 1999). Laboratory and field experiments have also demonstrated that DMS has a positive, dose-dependent response to solar radiation (Galí et al., 2013; Sunda et al., 2002; Vallina et al., 2007). In particular, gross DMS production is stimulated by ultra-violet radiation (UVR), which causes a reduction in algal cell integrity and enhanced release of DMSP, DMS, and cleavage enzymes, and also upregulation of intracellular DMSP cleavage (Galí et al., 2013). No relationship was observed between either $[DMS_{SSM}]$ or $[DMS_{6.0\,m}]$ with incident solar radiation in the current study, although this was confounded by differences in other factors such as phytoplankton biomass and community composition. The SSM was often sampled in the morning (08:00–09:30), which may suggest that the high DMS EFs in B1 may be a response to a night–day change in irradiance. Rapid changes in light can stimulate intracellular and dissolved DMSP production in coccolithophores (Darroch et al., 2015), with low-light cultures exposed to irradiance (including UVR) exhibiting an increase of 24–62 nmol L^{-1} h^{-1} DMS (Archer et al., 2010). These production rates are still 1–2 orders of magnitude lower than many of the calculated PR_{SSM} for B1 (Table 1), but nevertheless confirm the potential for rapid DMS accumulation in response to increased light stress. Deck board incubations of SSM and SSSW from B2 and B3 stations showed that DMS production in the light was approximately double that in the dark (Cliff Law, personal communication, 2016), consistent with other reports (Galí et al., 2013). The highest net production rate of 3.7 nmol L^{-1} h^{-1} in the light (Cliff Law, personal communication, 2016) was again substantially lower than the calculated PR_{SSM} in Table 1. Bacterial inhibition by high summertime UVR in the SSM (Zemmelink et al., 2006; Slezak et al., 2007) can decouple DMS production and consumption, with increased DMS observed in sub-surface waters (Vila-Costa et al., 2008). The coincidence of elevated phytoplankton DMS production, inhibition of bacterial DMSP consumption, and tolerance of bacterial DMSP degradation under elevated UV-A reported for BATS (Levine et al., 2012), provides further support for potential DMS accumulation in the SSM. However, the absence of a significant difference in DMSP cycling between light and dark incubations of SSSW during SOAP (Lizotte et al., 2016) suggests bacterial oxidation was not inhibited by light, although this was not measured in the SSM.

The different phytoplankton community composition of the three blooms may have influenced DMS enrichment in the SSM, particularly as all the blooms contained phytoplankton that are significant DMSP producers. B2 and B3 contained a higher proportion of coccolithophores but, despite evidence of their increased production of DMS and DMSP under high light stress (Archer et al., 2010), DMS levels were low in these two blooms. Conversely, B1 was dominated by dinoflagellates (> 50 % of the phytoplankton biomass) and $[DMS_{SSSW}]$ levels and SSM enrichment were significantly higher. Dinoflagellates are significant DMSP producers, with intracellular DMSP content and DMSP lyase activity that generally exceeds that reported for coccolithophores (Caruana and Malin, 2014). Enzymatic cleavage of DMSP is currently viewed as the primary process for DMS production, and dinoflagellates have been identified as capable of converting DMSP to DMS (Steinke et al., 2002, and references within). An association between elevated DMS and dinoflagellate biomass has been observed by a number of empirical studies (e.g. Zhang et al., 2014; Zindler et al., 2012).

Of the four dominant dinoflagellate species observed in B1, *Gyrodinium* has been reported in association with high DMSP concentrations in the field (see Table 1, Caruana and Malin, 2014). Some dinoflagellate species migrate to the surface during the day, which influences the vertical distribution of associated DMSP and DMS. For example, a 10-fold increase in [DMS] was recorded due to diel vertical migration of a dinoflagellate bloom in the St. Lawrence River (Merzouk et al., 2004). Analysis of phytoplankton community composition at the B1 stations showed only one dinoflagellate genus, *Ceratium*, which was more abundant at 1–2 cm relative to 2 m (data not shown), although this family does not generally exhibit high intracellular DMSP.

The EC data provide further evidence of a contribution of near-surface DMS production to air–sea flux, notably the close coincidence of significant EC- and SSM-derived resid-

ual [DMS] during B1 (Fig. 5c). The validity of this evidence is in part dependent upon generation of robust k values from the COARE model. Comparison with observational DMS data sets has confirmed that the COARE gas transfer model is a good predictor of k for DMS in most conditions (Blomquist et al., 2006; Yang et al., 2011), including the SOAP voyage (Fig. 5b). A discrepancy with COARE has been reported under high winds ($> 11\,\mathrm{m\,s^{-1}}$) in the North Atlantic, with lower measured k values attributed to the suppression of turbulence due to wind–wave interaction, by Bell et al. (2013). In the current data analysis this suppression would result in a lower [DMS_{inf}], in contrast to the elevated values observed. In addition, the largest deviations between [DMS_{inf}] and [$DMS_{6.0\,m}$] during B1 occurred at mid-range wind speeds (6–8 $\mathrm{m\,s^{-1}}$, Fig. 6a), where Bell et al. (2013) found good agreement with COARE. Consequently previous analysis does not indicate any significant bias in the COARE parameterization that could account for the high [DMS_{inf}] during B1.

Spatial decoupling of airside and waterside measurements inevitably introduces error into the estimate of residual [DMS]. For example, Bell et al. (2015) identify a spatial offset between measurements of DMS flux and seawater DMS of up to 2 km during SOAP. However, this is unlikely to have generated the significant differences between [DMS_{inf}] and [$DMS_{6.0\,m}$] observed in B1, as these anomalies were observed when the ship was stationary or travelling slowly (< 2 knots), when wind speeds were $< 10\,\mathrm{m\,s^{-1}}$ (see Fig. 5a). During these conditions, the flux footprint (Bell et al., 2015) would be much smaller. In addition, [DMS_{inf}] exceeded $20\,\mathrm{nmol\,L^{-1}}$ on a number of occasions during B1, whereas [$DMS_{6.0\,m}$] rarely exceeded $20\,\mathrm{nmol\,L^{-1}}$ throughout the entire voyage, suggesting that horizontal transport of DMS in the marine boundary layer from another bloom was not the source of the anomalously high [DMS_{inf}] during B1.

5 Summary

Dimethylsulfide fluxes are traditionally computed using [DMS] at depths below the air–sea interface; consequently significant near-surface DMS has important implications for flux estimates. Sub-surface [DMS] between 1 and 160 cm depth was relatively uniform at all stations on the Chatham Rise, in contrast to suggestions that DMS concentration should decrease near the air–sea interface as a result of surface sinks (Kieber et al., 1996). Although near-surface DMS gradients were generally absent, a significant exception was recorded in a dinoflagellate bloom during light to mid-range wind speeds (i.e. $< 10\,\mathrm{m\,s^{-1}}$) and near-surface temperature stratification. On several occasions in this bloom, significant enrichment of DMS in the SSM coincided with measured DMS fluxes that exceeded predicted fluxes calculated using sub-surface [DMS] and the COARE algorithm. Although SSM enrichment of DMS (see Table 1) and anomalously high air–sea DMS fluxes have previously been reported (e.g. Marandino et al., 2008, 2007), this study's results are the first to link these two phenomena.

There are some aspects of this data set that are surprising and require further investigation to establish the significance of the SSM to air–sea DMS flux. For example, the study raises questions as to how significant DMS enrichment is maintained in the SSM without influencing the [DMS] in the underlying water. In addition, the elevated SSM [DMS], both measured and inferred from flux measurements in the dinoflagellate bloom B1, necessitates a substantial in situ DMS production in the SSM. To maintain this enrichment, DMS production is required at a rate that significantly exceeds previous estimates for the open ocean (Simó, 2004). Nevertheless, the two independent approaches used in this study indicate that the SSM may influence DMS air–sea flux under certain biogeochemical and meteorological conditions, and so production at the air–sea interface may contribute to anomalously high DMS fluxes recorded in other regions of high productivity (Marandino et al., 2009, 2008).

6 Data availability

The [$DMS_{6.0m}$] dataset can be downloaded from http://saga.pmel.noaa.gov/dms/select.php.

Author contributions. C. Walker designed and conducted the experiments, developed and optimized the analytical methods and instrument, analysed the SSM and 1.6 m depth seawater samples for DMS, and interpreted the data. C. Walker also prepared the manuscript with contributions from C. Law, M. Harvey, M. Smith, and T. Bell. C. Law helped with the experimental design, instrument optimization, sample collection, data interpretation, and drafting of the manuscript. C. Law also assisted with sampling logistics and coordinated the overall measurement programme through his role as voyage leader. M. Harvey and J. McGregor assisted in the development of the analytical instrument, as did A. Marriner, who also helped with the collection and analysis of seawater DMS samples. C. Law, M. Harvey, and M. Smith provided invaluable mentoring and assisted with data interpretation and analysis. T. Bell and E. Saltzman supplied the air–sea DMS flux and miniCIMS seawater DMS data, and contributed to data interpretation.

Acknowledgements. The authors thank Captain Evan Solly and the crew of the R/V *Tangaroa* for their invaluable assistance with the field component of this study. We also thank Kim Currie (NIWA, Otago), Martine Lizotte (Laval University), Fiona Elliott (NIWA), and Karl Safi (NIWA, Hamilton) for their help in the collection and analysis of seawater samples and measurements, and Christa Marandino, Warren DeBruyn, and Cyril McCormick for their assistance with the supporting CIMS measurements. This research was supported by funding from NIWA's Climate and Atmosphere Research Programme 3 – role of the oceans (2015/16 SCI), and a New Zealand Ministry for Business, Innovation, and Employment (MBIE) Postdoctoral Fellowship (award number

CO1X0911). Thomas G. Bell and Eric S. Saltzman were supported by the NSF Atmospheric Chemistry Program (grant nos. 08568, 0851472, 0851407, and 1143709).

Edited by: M. Hoppema
Reviewed by: two anonymous referees

References

Agogué, H., Casamayor, E. O., Joux, F., Obernosterer, I., Dupuy, C., Lantoine, F., Catala, P., Weinbauer, M. G., Reinthaler, T., Herndl, G. J., and Lebaron, P.: Comparison of samplers for the biological characterization of the sea-surface microlayer, Limnol. Oceanogr.-Meth., 2, 213–225, 2004.

Andreae, M. O. and Crutzen, P. J.: Atmospheric aerosols: Biogeochemical sources and role in atmospheric chemistry, Science, 276, 1052–1058, 1997.

Archer, S. D., Ragni, M., Webster, R., Airs, R. L., and Geider, R. J.: Dimethyl sulfoniopropionate and dimethyl sulfide production in response to photoinhibition in Emiliania huxleyi, Limnol. Oceanogr., 55, 1579–1589, 2010.

Asher, W. E., Karle, L. M., Higgins, B. J., Farley, P. J., Monahan, E. C., and Leifer, I. S.: The influence of bubble plumes on air-seawater gas transfer velocities, J. Geophys. Res.-Ocean., 101, 12027–12041, 1996.

Ayers, G. P. and Gillett, R. W.: DMS and its oxidation products in the remote marine atmosphere: implications for climate and atmospheric chemistry, J. Sea Res., 43, 275–286, 2000.

Bandy, A. R., Thornton, D. C., Tu, F. H., Blomquist, B. W., Nadler, W., Mitchell, G. M., and Lenschow, D. H.: Determination of the vertical flux of dimethyl sulfide by eddy correlation and atmospheric pressure ionization mass spectrometry (APIMS), J. Geophys. Res.-Atmos., 107, 4743, doi:10.1029/2002jd002472, 2002.

Bell, T. G., De Bruyn, W. J., Miller, S. D., Ward, B., Christensen, K. H., and Saltzman, E. S.: Air-sea dimethylsulfide (DMS) gas transfer in the North Atlantic: Evidence for limited interfacial gas exchange at high wind speed, Atmos. Chem. Phys., 13, 11073–11087, 2013.

Bell, T. G., De Bruyn, W., Miller, S. D., Ward, B., Christensen, K. H., and Saltzman, E. S.: Air–sea dimethylsulfide (DMS) gas transfer in the North Atlantic: evidence for limited interfacial gas exchange at high wind speed, Atmos. Chem. Phys., 13, 11073–11087, doi:10.5194/acp-13-11073-2013, 2013.

Bianchi, F., Trostl, J., Junninen, H., Frege, C., Henne, S., Hoyle, C. R., Molteni, U., Herrmann, E., Adamov, A., Bukowiecki, N., Chen, X., Duplissy, J., Gysel, M., Hutterli, M., Kangasluoma, J., Kontakanen, J., Kurten, Al, Manninen, H. E., Munch, S., Perakyla, O., Petaja, T., Rondo, L., Williamson, C., Weingartner, E., Curtius, J., Worsnop, D. R., Kulmala, M., Dommen, J., and Baltensperger, U.: New particle formation in the free troposphere: A question of chemistry and timing, Science, 352, 1109–1112, 2016.

Blomquist, B. W., Fairall, C. W., Huebert, B. J., Kieber, D. J., and Westby, G. R.: DMS sea-air transfer velocity: Direct measurements by eddy covariance and parameterization based on the NOAA/COARE gas transfer model, Geophys. Res. Lett., 33, L07601, doi:10.1029/2006GL025735, 2006.

Calleja, M. L., Duarte, C. M., Navarro, N., and Agustí, S.: Control of air-sea CO_2 disequilibria in the subtropical NE Atlantic by planktonic metabolism under the ocean skin, Geophys. Res. Lett., 32, L08606, doi:10.1029/2004GL022120, 2005.

Carlson, D. J.: Dissolved organic materials in surface microlayers: temporal and spatial variability and relation to sea state, Limnol. Oceanogr., 28, 415–431, 1983.

Caruana, A. M. N. and Malin, G.: The variability in DMSP content and DMSP lyase activity in marine dinoflagellates, Prog. Oceanogr., 120, 410–424, 2014.

Charlson, R. J., Lovelock, J. E., Andreae, M. O., and Warren, S. G.: Oceanic phytoplankton, atmospheric sulphur, cloud albedo and climate, Nature, 326, 655–661, 1987.

Cunliffe, M. and Wurl, O.: Guide to Best Practices to Study the Ocean's Surface, Occasional Publications of the Marine Biological Association of the United Kingdom, 118 pp., 2014.

Cunliffe, M., Engel, A., Frka, S., Gašparović, B., Guitart, C., Murrell, J. C., Salter, M., Stolle, C., Upstill-Goddard, R., and Wurl, O.: Sea-surface microlayers: A unified physicochemical and biological perspective of the air–ocean interface, Prog. Oceanogr., 109, 104–116, 2013.

Dacey, J. W. H., Wakeham, S. G., and Howes, B. L.: Henry's law constants for dimethylsulfide in fresh-water and seawater, Geophys. Res. Lett., 11, 991–994, 1984.

Darroch, L. J., Lavoie, M., Levasseur, M., Laurion, I., Sunda, W. G., Michaud, S., Scarratt, M., Gosselin, M., and Caron, G.: Effect of short-term light- and UV-stress on DMSP, DMS, and DMSP lyase activity in Emiliania huxleyi, Aquat. Microb. Ecol., 74, 173–185, 2015.

Edson, J. B., Hinton, A. A., Prada, K. E., Hare, J. E., and Fairall, C. W.: Direct covariance flux estimates from mobile platforms at sea, J. Atmos. Ocean. Tech., 15, 547–562, 1998.

Fairall, C. W., Yang, M., Bariteau, L., Edson, J. B., Helmig, D., McGillis, W., Pezoa, S., Hare, J. E., Huebert, B., and Blomquist, B.: Implementation of the Coupled Ocean-Atmosphere Response Experiment flux algorithm with CO_2, dimethylsulfide, and O_3, J. Geophys. Res.-Ocean., 116, C00F09, doi:10.1029/2010JC006884, 2011.

Galí, M., Simó, R., Pérez, G. L., Fuentes-Lema, A., Gasol, J. M., Royer, S. J., Ruiz-González, C., and Sarmento, H.: Differential response of planktonic primary, bacterial, and dimethylsulfide production rates to static vs. dynamic light exposure in upper mixed-layer summer sea waters, Biogeosciences, 10, 7983–7998, doi:10.5194/bg-10-7983-2013, 2013.

Garrett, W. D.: Collection of slick-forming materials from the sea-surface, Limnol. Oceanogr., 10, 602–605, 1965.

Harvey, G. W.: Microlayer collection from the sea-surface: A method and initial results, Limnol. Oceanogr., 11, 608–613, 1966.

Harvey, G. W. and Burzell, L. A.: A simple microlayer method for small samples, Limnol. Oceanogr., 17, 156–157, 1972.

Ho, D. T., Asher, W. E., Bliven, L. F., Schlosser, P., and Gordan, E. L.: On mechanisms of rain-induced air-water gas exchange, J. Geophys. Res.-Ocean., 105, 24045–24057, 2000.

Ho, D. T., Law, C. S., Smith, M. J., Schlosser, P., Harvey, M., and Hill, P.: Measurements of air-sea gas exchange at high wind speeds in the Southern Ocean: implications for global parameterizations, Geophys. Res. Lett., 33, L16611, doi:10.1029/2006GL026817, 2006.

Ho, D. T., Wanninkhof, R., Schlosser, P., Ullman, D. S., Hebert, D., and Sullivan, K. F.: Toward a universal relationship between wind speed and gas exchange: Gas transfer velocities measured with ^3He / SF_6 during the Southern Ocean Gas Exchange Experiment, J. Geophys. Res.-Ocean., 116, C00F04, doi:10.1029/2010jc006854, 2011.

Huebert, B. J., Blomquist, B. W., Hare, J. E., Fairall, C. W., Johnson, J. E., and Bates, T. S.: Measurement of the sea-air DMS flux and transfer velocity using eddy correlation, Geophys. Res. Lett., 31, L23113, doi:10.1029/2004GL021567, 2004.

Kettle, A. J. and Andreae, M. O.: Flux of dimethylsulfide from the oceans: A comparison of updated data sets and flux models, J. Geophys. Res.-Atmos., 105, 26793–26808, 2000.

Kieber, D. J., Jiao, J. F., Kiene, R. P., and Bates, T. S.: Impact of dimethylsulfide photochemistry on methyl sulfur cycling in the equatorial Pacific Ocean, J. Geophys. Res.-Ocean., 101, 3715–3722, 1996.

Kirkby, J., Duplissy, J., Sengupta, K., Frege, C., Gordon, H., Williamson, C., Heinritzi, M., Simon, M., Yan, C., Almeida, J., Tröstl, J., Nieminen, T., Ortega, I. K., Wagner, R., Adamov, A., Amorim, A., Bernhammer, A. K., Bianchi, R., Breitenlechner, M., Brilke, S., Chen, X., Craven, J., Dias, A., Ehrhart, S., Flagan, R. C., Franchin, A., Fuchs, C., Guida, R., Hakala, J., Hoyle, C. R., Jokinen, T., Junninen, H., Kangasluoma, J., Kim, J., Krapf, M., Kürten, A., Laaksonen, A., Lehtipalo, K., Makhmutov, V., Mathot, S., Molteni, U., Onnela, A., Peräkylä, O., Piel, F., Petäjä, T., Praplan, A. P., Pringle, K., Rap, A., Richards, N. A. D., Riipinen, I., Rissanen, P., Rondo, L., Sarnela, N., Schobesberger, S., Scott, C. E., Seinfeld, J. H., Sipilä, M., Steiner, G., Stozhkov, Y., Stratmann, F., Tomé, A., Virtanen, A., Vogel, A. L., Wagner, A. C., Wagner, P. E., Weingartner, E., Wimmer, D., Winkler, P. M., Ye, P., Zhang, X., Hansel, A., Dommen, J., Donahue, N. M., Worsnop, D. R., Baltensperger, U., Kulmala, M., Carslaw, K. S., and Curtius, J.: Ion-induced nucleation of pure biogenic particles, Nature, 533, 521–526, 2016.

Lana, A., Bell, T. G., Simo, R., Vallina, S. M., Ballabrera-Poy, J., Kettle, A. J., Dachs, J., Bopp, L., Saltzman, E. S., Stefels, J., Johnson, J. E., and Liss, P. S.: An updated climatology of surface dimethlysulfide concentrations and emission fluxes in the global ocean, Global Biogeochem. Cy., 25, GB1004, doi:10.1029/2010gb003850, 2011.

Law, C. S., Smith, M. J., Walker, C. F., Currie, K., Bell, T. G., Saltzman, E. S., and Harvey, M. J.: An overview of the Southern Ocean Aerosol Production (SOAP) voyage, Atmos. Phys. Chem., in preparation, 2016.

Levine, N. M., Varaljay, V. A., Toole, D. A., Dacey, J. W., Doney, S. C., and Moran, M. A.: Environmental, biochemical and genetic drivers of DMSP degradation and DMS production in the Sargasso Sea, Environ. Microbiol., 14, 1210–1223, 2012.

Liss, P. S.: Gas transfer: Experiments and geochemical implications, in: Air-Sea Exchange of Gases and Particles, edited by: Liss, P. S. and Slinn, W. G. N., NATO ASI Series, Springer Netherlands, 241–298, 1983.

Liss, P. S. and Duce, R. A.: The Sea-surface and Global Change, in: Cambridge University Press, edited by: Liss, P. S. and Duce, R. A., available at: doi:10.1017/CBO9780511525025, Cambridge Books Online, Cambridge, 1997.

Liss, P. S. and Merlivat, L.: Air–sea gas exchange rates: Introduction and synthesis, in: The Role of Air-Sea Exchange in Geochemical Cycling, edited by: Buat-Ménard, P., NATO ASI Series, Springer Netherlands, 113–127, 1986.

Liss, P. S. and Slater, P. G.: Flux of gases across the air-sea interface, Nature, 247, 181–184, doi:10.1038/247181a0, 1974.

Lizotte, M., Levasseur, M., Law, C. S., Safi, K., Marriner, A., and Kiene, R. P.: Converging facets of oceanic dimethylsulfoniopropionate (DMSP) and dimethylsufide (DMS) bacterial cycling across biological hotspots of the New Zealand Subtropical Front, Ocean Sci., in preparation, 2016.

Marandino, C. A., De Bruyn, W. J., Miller, S. D., and Saltzman, E. S.: Eddy correlation measurements of the air/sea flux of dimethylsulfide over the North Pacific Ocean, J. Geophys. Res.-Atmos., 112, D03301, doi:10.1029/2006jd007293, 2007.

Marandino, C. A., De Bruyn, W. J., Miller, S. D., and Saltzman, E. S.: DMS air/sea flux and gas transfer coefficients from the North Atlantic summertime coccolithophore bloom, Geophys. Res. Lett., 35, L23812, doi:10.1029/2008gl036370, 2008.

Marandino, C. A., De Bruyn, W. J., Miller, S. D., and Saltzman, E. S.: Open ocean DMS air/sea fluxes over the eastern South Pacific Ocean, Atmos. Chem. Phys., 9, 345–356, doi:10.5194/acp-9-345-2009, 2009.

Matrai, P. A., Tranvik, L., Leck, C., and Knulst, J. C.: Are high Arctic surface microlayers a potential source of aerosol organic precursors?, Mar. Chem., 108, 109–122, 2008.

McCoy, D. T., Burrows, S. M., Wood, R., Grosvenor, D. P., Elliott, S. M., Ma, P.-L., Rasch, P. J., and Hartmann, D. L.: Natural aerosols explain seasonal and spatial patterns of Southern Ocean cloud albedo, Sci. Adv., 1, doi:10.1126/sciadv.1500157, 2015.

McGillis, W. R., Dacey, J. W. H., Frew, N. M., Bock, E. J., and Nelson, R. K.: Water-air flux of dimethylsulfide, J. Geophys. Res.-Ocean., 105, 1187–1193, 2000.

Merzouk, A., Levasseur, M., Scarratt, M., Michaud, S., and Gosselin, M.: Influence of dinoflagellate diurnal vertical migrations on dimethylsulfoniopropionate and dimethylsulfide distribution and dynamics (St. Lawrence Estuary, Canada), Can. J. Fish. Aquat. Sci., 61, 712–720, 2004.

Momzikoff, A., Brinis, A., Dallot, S., Gondry, G., Saliot, A., and Lebaron, P.: Field study of the chemical characterization of the upper ocean surface using various samplers, Limnol. Oceanogr.-Meth., 2, 374–386, 2004.

Murphy, R. J., Pinkerton, M. H., Richardson, K. M., Bradford-Grieve, J. M., and Boyd, P. W.: Phytoplankton distributions around New Zealand derived from SeaWiFS remotely-sensed ocean colour data, New Zeal. J. Mar. Fresh., 35, 343–362, 2001.

Nguyen, B. C., Gaudrey, A., Bonsang, B., and Lambert, G.: Reevaluation of the role of dimethly sulphide in the sulphur budget, Nature, 275, 637–639, 1978.

Nightingale, P. D.: Air–sea gas exchange, in: Surface Ocean–Lower Atmosphere Processes, edited by: Le Quéré, C. and Saltzman, E. S., American Geophysical Union, 69–97, 2013.

Nightingale, P. D., Liss, P. S., and Schlosser, P.: Measurements of air-sea gas transfer during an open ocean algal bloom, Geophys. Res. Lett., 27, 2117–2120, 2000.

Quinn, P. K. and Bates, T. S.: The case against climate regulation via oceanic phytoplankton sulphur emissions, Nature, 480, 51–56, 2011.

Salter, M. E., Upstill-Goddard, R. C., Nightingale, P. D., Archer, S. D., Blomquist, B., Ho, D. T., Huebert, B., Schlosser, P., and Yang, M.: Impact of an artificial surfactant release on air-sea gas

fluxes during Deep Ocean Gas Exchange Experiment II, J. Geophys. Res.-Ocean., 116, C11016, doi:10.1029/2011JC007023, 2011.

Saltzman, E. S., King, D. B., Holmen, K., and Leck, C.: Experimental determination of the diffusion coefficient of dimethylsulfide in water, J. Geophys. Res.-Ocean., 98, 16481–16486, 1993.

Schmidt, R. and Schneider, B.: The effect of surface films on the air–sea gas exchange in the Baltic Sea, Mar. Chem., 126, 56–62, 2011.

Simó, R.: Production of atmospheric sulfur by oceanic plankton: Biogeochemical, ecological and evolutionary links, Trends Ecol. Evol., 16, 287–294, 2001.

Simó, R.: From cells to globe: approaching the dynamics of DMS(P) in the ocean at multiple scales, Can. J. Fish. Aquat. Sci., 61, 673–684, 2004.

Simó, R. and Pedrós-Alió, C.: Short-term variability in the open ocean cycle of dimethylsulfide, Global Biogeochem. Cy., 13, 1173–1181, 1999.

Slezak, D., Kiene, R. P., Toole, D. A., Simó, R., and Kieber, D. J.: Effects of solar radiation on the fate of dissolved DMSP and conversion to DMS in seawater, Aquat. Sci., 69, 377–393, 2007.

Steinke, M., Marlin, G., Archer, S. D., Burkill, P. H., and Liss, P. S.: DMS production in a coccoltihophorid bloom: evidence for the importance of dinoflagellate DMSP lyases, Aquat. Microb. Ecol., 26, 259–70, 2002.

Sunda, W., Kieber, D. J., Kiene, R. P., and Huntsman, S.: An antioxidant function for DMSP and DMS in marine algae, Nature, 418, 317–320, 2002.

Swan, H. B., Armishaw, P., Iavetz, R., Alamgir, M., Davies, S. R., Bell, T. G., and Jones, G. B.: An interlaboratory comparison for the quantification of aqueous dimethylsulphide, Limnol. Oceanogr.-Meth., 12, 784–794, 2014.

Sweeney, C., Gloor, E., Jacobson, A. R., Key, R. M., McKinley, G., Sarmiento, J. L., and Wanninkhof, R.: Constraining global air-sea gas exchange for CO_2 with recent bomb ^{14}C measurements, Global Biogeochem. Cy., 21, GB2015, doi:10.1029/2006GB002784, 2007.

Swinbank, W. C.: The measurement of vertical transfer of heat and water vapor by eddies in the lower atmosphere, J. Meteorol., 8, 135–145, 1951.

Toole, D. A. and Siegel, D. A.: Light-driven cycling of dimethylsulfide (DMS) in the Sargasso Sea: closing the loop, Geophys. Res. Lett., 31, L09308, doi:10.1029/2004GL019581, 2004.

Turner, S. M. and Liss, P. S.: Measurements of various sulphur gases in a coastal marine environment, J. Atmos. Chem., 2, 223–232, 1985.

Turner, S. M., Malin, G., Liss, P. S., Harbour, D. S., and Holligan, P. M.: The seasonal variation of dimethyl sulfide and dimethylsulfoniopropionate concentrations in nearshore waters, Limnol. Oceanogr., 33, 364–375, 1988.

Vallina, S. M., Simo, R., Gasso, S., De Boyer-Montegut, C., del Rio, E., Jurado, E., and Dachs, J.: Analysis of a potential "solar radiation dose-dimethylsulfide-cloud condensation nuclei" link from globally mapped seasonal correlations, Global Biogeochem. Cy., 21, GB2004, doi:10.1029/2006GB002787, 2007.

Vila-Costa, M., Kiene, R. P., and Simó, R.: Seasonal variability of the dynamics of dimethylated sulfur compounds in a coastal northwest Mediterranean site, Limnol. Oceanogr., 53, 198–211, 2008.

Walker, C. F., Harvey, M. J., Bury, S. J., and Chang, F. H.: Biological and physical controls on dissolved dimethylsulfide over the north-eastern continental shelf of New Zealand, J. Sea Res., 43, 253–264, 2000.

Wanninkhof, R.: Relationship between Wind-Speed and Gas-Exchange over the Ocean, J. Geophys. Res.-Ocean., 97, 7373–7382, 1992.

Wanninkhof, R., Sullivan, K. F., and Top, Z.: Air-sea gas transfer in the Southern Ocean, J. Geophys. Res.-Ocean., 109, C08S19, doi:10.1029/2003JC001767, 2004.

Wolfe, G. V., Strom, S. L., Holmes, J. L., Radzio, T., and Olson, M. B.: Dimethylsulfoniopropionate cleavage by marine phytoplankton in response to mechanical, chemical, or dark stress, J. Phycol., 38, 948–960, 2002.

Woolf, D. K.: Parametrization of gas transfer velocities and sea-state-dependent wave breaking, Tellus B, 57, 87–94, 2005.

Wurl, O., Wurl, E., Miller, L., Johnson, K., and Vagle, S.: Formation and global distribution of sea-surface microlayers, Biogeosciences, 8, 121–135, doi:10.5194/bg-8-121-2011, 2011.

Yang, G. P.: Dimethylsulfide enrichment in the surface microlayer of the South China Sea, Mar. Chem., 66, 215–224, 1999.

Yang, G. P. and Tsunogai, S.: Biogeochemistry of dimethylsulfide (DMS) and dimethylsulfoniopropionate (DMSP) in the surface microlayer of the western North Pacific, Deep-Sea Res. Pt. I, 52, 553–567, 2005.

Yang, G. P., Watanabe, S., and Tsunogai, S.: Distribution and cycling of dimethylsulfide in surface microlayer and subsurface seawater, Mar. Chem., 76, 137–153, 2001.

Yang, G. P., Levasseur, M., Michaud, S., and Scarratt, M.: Biogeochemistry of dimethylsulphide (DMS) and dimethylsulfoniopropionate (DMSP) in the surface microlayer and sub-surface water of the western North Atlantic during spring, Mar. Chem., 96, 315–329, 2005a.

Yang, G. P., Tsunogai, S., and Watanabe, S.: Biogenic sulfur distribution and cycling in the surface microlayer and sub-surface water of Funka Bay and its adjacent area, Cont. Shelf Res., 25, 557–570, 2005b.

Yang, G. P., Jing, W.-W., Li, L., Kang, Z.-Q., and Song, G.-S.: Distribution of dimethylsulphide and dimethylsulfoniopropionate in the surface microlayer and sub-surface water of the Yellow Sea, China during spring, J. Mar. Syst., 62, 22–34, 2006.

Yang, G. P., Jing, W.-W., Kang, Z.-Q., Zhang, H.-H., and Song, G.-S.: Spatial variations of dimethylsulphide and dimethylsulfoniopropionate in the surface microlayer and in the sub-surface waters of the South China Sea during springtime, Mar. Environ. Res., 65, 85–97, 2008.

Yang, G. P., Levasseur, M., Michaud, S., Merzouk, A., Lizotte, M., and Scarratt, M.: Distribution of dimethylsulphide and dimethylsulfoniopropionate and its relation with phytoneuston in the surface microlayer of the western North Atlantic during summer, Biogeochemistry, 94, 243–254, 2009.

Yang, M., Blomquist, B. W., Fairall, C. W., Archer, S. D., and Huebert, B. J.: Air-sea exchange of dimethylsulfide in the Southern Ocean: Measurements from SO GasEx compared to temperate and tropical regions, J. Geophys. Res.-Ocean., 116, C00F05, doi:10.1029/2010JC006526, 2011.

Yoch, D. C.: Dimethylsulfoniopropionate: Its sources, role in the marine food web, and biological degradation to dimethylsulfide, Appl. Environ. Microbiol., 68, 5804–5815, 2002.

Zemmelink, H. J., Dacey, J. W. H., and Hintsa, E. J.: Direct measurements of biogenic dimethylsulfide fluxes from the oceans: a synthesis, Can. J. Fish. Aquat. Sci., 61, 836–844, 2004.

Zemmelink, H. J., Houghton, L., Sievert, S. M., Frew, N. M., and Dacey, J. W. H.: Gradients in dimethylsufide, dimethylsulfoniopropionate, dimethylsulfoxide, and bacteria near the sea-surface, Mar. Ecol.-Prog. Ser., 295, 33–42, 2005.

Zemmelink, H. J., Houghton, L., Frew, N. M., and Dacey, J. W. H.: Dimethylsulfide and major sulfur compounds in a stratified coastal salt pond, Limnol. Oceanogr., 51, 271–279, 2006.

Zhang, H. H., Yang, G. P., and Zhu, T.: Distribution and cycling of dimethylsulphide (DMS) and dimethylsulfoniopropionate (DMSP) in the sea-surface microlayer of the Yellow Sea, China, in spring, Cont. Shelf Res., 28, 2417–2427, 2008.

Zhang, H. H., Yang, G. P., Liu, C. Y., and Li, C. X.: Seasonal variations of dimethylsulphide (DMS) and dimethylsulfoniopropionate (DMSP) in the sea-surface microlayer and sub-surface water of Jiaozhou Bay and its adjacent area, Acta Oceanol. Sin., 28, 73–86, 2009.

Zhang, S. H., Yang, G. P., Zhang, H. H., and Yang, J.: Spatial variation of biogenic sulfur in the south Yellow Sea and the East China Sea during summer and its contribution to atmospheric sulfate aerosol, Sci. Total Environ., 488/489, 157–167, 2014.

Zhang, Z., Liu, L., Liu, C., and Cai, W.: Studies on the sea-surface microlayer: II. The layer of sudden change of physical and chemical properties, J. Colloid Interf. Sci., 264, 148–159, 2003.

Zindler, C., Peeken, I., Marandino, C. A., and Bange, H. W.: Environmental control on the variability of DMS and DMSP in the Mauritanian upwelling region, Biogeosciences, 9, 1041–1051, doi:10.5194/bg-9-1041-2012, 2012.

Zuev, B., Chudinova, V., Kovalenko, V., and Yagov, V.: The conditions of formation of the chemical composition of the sea-surface microlayer and techniques for studying organic matter in it, Geochem. Int. Geokhimiia, 39, 702–710, 2001.